Journal of The Electrochemical Society, **156** (12) K215-K217 (2009)
0013-4651/2009/156(12)/K215/3/$25.00 © The Electrochemical Society

Internal Strain Distribution in Freestanding Porous Silicon

Y. A. Pusep,[a,z] A. D. Rodrigues,[b] J. C. Galzerani,[b] R. D. Arce,[c] R. R. Koropecki,[c] and D. Comedi[d]

[a]*Instituto de Fisica de São Carlos, Universidade de São Paulo, 13560-970 São Carlos, SP, Brazil*
[b]*Departamento de Física, Universidade Federal de São Carlos, 13565-905 São Carlos, SP, Brazil*
[c]*Instituto de Desarrollo Tecnológico para la Industria Química (INTEC), Consejo Nacional de Investigaciones Cientificas y Técnicas (CONICET), Universidad Nacional del Litoral (UNL), 3000 Santa Fe, Argentina*
[d]*Laboratorio de Física del Sólido (LAFISO) and CONICET, Departamento de Física, Facultad de Ciencias Exactas y Tecnología (FACET), Universidad Nacional de Tucumán, 4000 Tucumán, Argentina*

Elastic properties of freestanding porous silicon layers fabricated by electrochemical anodization were studied by Raman scattering. Different anodization currents provided different degrees of porosity in the nanometer scale. Raman lines corresponding to the longitudinal optical phonons of crystalline and amorphous phases were observed. The amorphous volume fraction increased and the phonon frequencies for both phases decreased with increasing porosity. A strain distribution model is proposed whose fit to the experimental results indicates that the increasing nanoscale porosity causes strain relaxation in the amorphous domains and strain buildup in the crystalline ones. The present analysis has significant implications on the estimation of the crystalline Si domain's characteristic size from Raman scattering data.
 [DOI: 10.1149/1.3225832]

Manuscript submitted December 15, 2008; revised manuscript received August 19, 2009. Published October 1, 2009.

Porous silicon (P-Si) is a class of nanostructured Si with promising applications in optoelectronic devices because of its strong visible photoluminescence and its compatibility with Si device technology. Moreover, the P-Si structure is of much fundamental scientific interest because of its fractal characteristics. Particularly, P-Si has been used as a model system to investigate relationships between pore structure and elastic properties, which constitute an important problem related to the propagation of waves in composite elastic media (see Ref. 1 and references therein). In this regard, P-Si represents a valuable tool because of its controlled porosity. The vibrational properties of P-Si were extensively studied by Raman scattering of the optical phonons. It was shown that the shape and the peak position of the main Raman line are determined by the spatial confinement of the optical phonons in Si nanocrystals that result from the etching of the crystalline Si wafer that is involved in the P-Si fabrication process.[2-4] Using the theory developed in Ref. 5 and 6, the average size of the confinement regions characterizing the porous structure can be obtained. However, the applicability of Raman scattering for the characterization of the nanostructured silicon was questioned in Ref. 7 for cases where the strain in the sample is not independently known. The importance of the external (related to the lattice parameter mismatch between the substrate and the porous film) and internal (resulting from internal interfaces and observed in freestanding P-Si films) strains in the determination of the corresponding Raman line positions has also been indicated in Ref. 8-11. A possible source of internal strain is the natural oxidation of the pore surfaces, as it is well known that the Si/SiO_2 interface is considerably strained.[12,13] In this regard, however, the role of the amorphous Si (a-Si) domains that often form, probably on the pore surfaces, as a result of the etching process in the fabrication of P-Si,[14,15] has generally been overlooked.

In this work we study the Raman scattering by optical phonons in freestanding P-Si samples with varying porosity. The Raman spectra show clear contributions due to crystalline and amorphous domains and the amorphous phase volume fraction increasing with increasing porosity. The analysis of the strain distribution over the two phases allows for a separate determination of the contributions due to the confinement and strain effects to the Raman shift of the phonon frequency related to the crystalline phase. This results in a considerable correction in the determination of the characteristic size of the crystalline Si domains.

[z] E-mail: pusep@ifsc.usp.br

Self-supported P-Si layers were prepared by electrochemical anodization of p-type boron-doped (1–4 MΩ cm resistivity) silicon wafers in a similar way as in Ref. 14. Different anodization currents (from 12 to 128 mA/cm^2) provided different degrees of porosity (from 50 to 90% as determined from reflectance measurements) with characteristic pore sizes in the nanometer scale. Figure 1 shows a scanning electron microscope (SEM) image of one of the studied samples, which demonstrates the formation of the porous structure in the selected sample in the nanometer scale. To characterize the porosity, reflectance spectra in the visible range were fitted within an effective medium approximation using the Looyenga mixing rule[16,17] to calculate the complex refractive index for each anodization current, as a function of the wavelength. The fitting parameters for each sample were the sample thickness and the porosity. The porosity obtained in this way as a function of the anodization current density is shown in Fig. 2. A linear behavior is observed in a wide current density range.

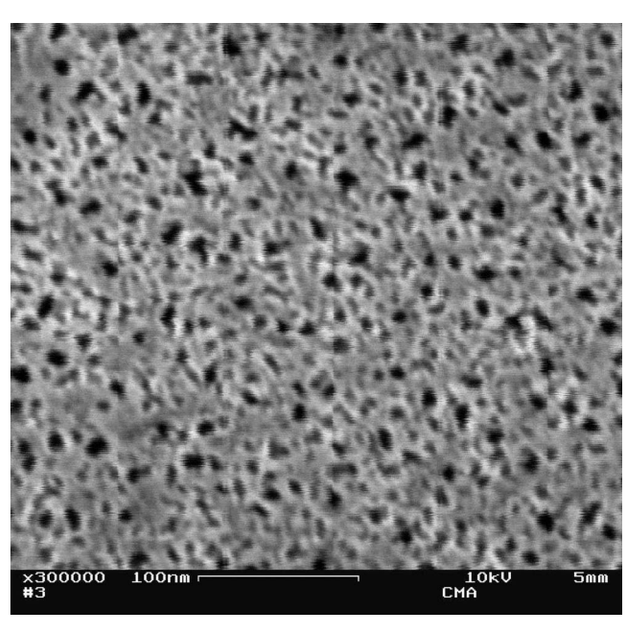

Figure 1. SEM image of porous Si fabricated with an anodization current of 12 mA/cm^2.

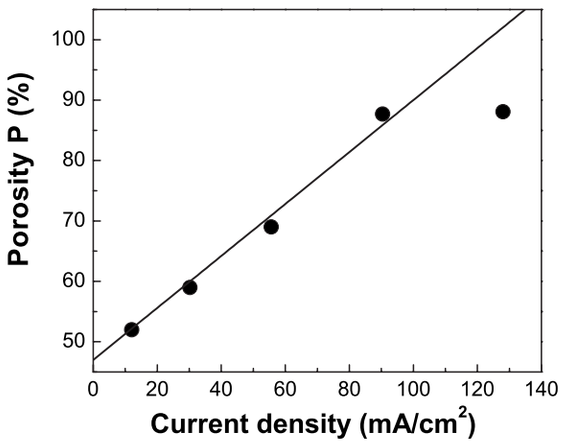

Figure 2. Porosity of P-Si samples fabricated with different anodization current densities.

Raman scattering was collected from the surface of the samples at $T = 10$ K in the backscattering configuration with an Instruments S.A. T64000 triple grating spectrometer supplied with a liquid-nitrogen-cooled charge-coupled device detector. The 5145 Å line of an Ar^+ laser was used for nonresonant excitation.

Raman scattering from all studied samples revealed the low frequency and high frequency lines caused by the longitudinal optical (LO) phonons in the a-Si and crystalline (c-Si) phases, respectively. We did not find any noticeable evidence of SiO_2. Therefore, we conclude that in the samples studied here the contribution from natural SiO_2 is small as compared to those due to the a-Si and c-Si phases and is consequently neglected in the following analysis.

A typical Raman scattering spectrum from one of the samples is shown in Fig. 3. The amorphous fraction was determined using the integrated Raman intensity of the amorphous (I_a) to the crystalline (I_c) components ratio normalized by the Raman cross sections for a-Si and c-Si, respectively, assuming a cross-section normalization factor of 0.14 (corresponding to the excitation energy of 2.4 eV) as in Ref. 18 and 19. The obtained data demonstrate a considerable

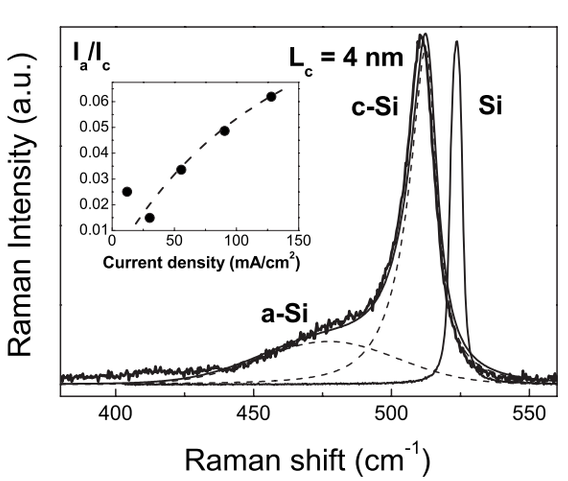

Figure 3. Raman scattering spectra measured at $T = 10$ K in the optical phonon frequency range from a P-Si sample produced at a current density of $j = 128$ mA/cm^2. The solid line is the result of a model fitting. Dashed lines show the contributions of the a- and c-Si phases. The Raman line corresponding to the LO phonon of the Si substrate (Si) is also shown. The inset shows the amorphous (I_a) to crystalline (I_c) integrated Raman intensity components ratio as a function of the anodization current. The dashed line is a guide for the eyes.

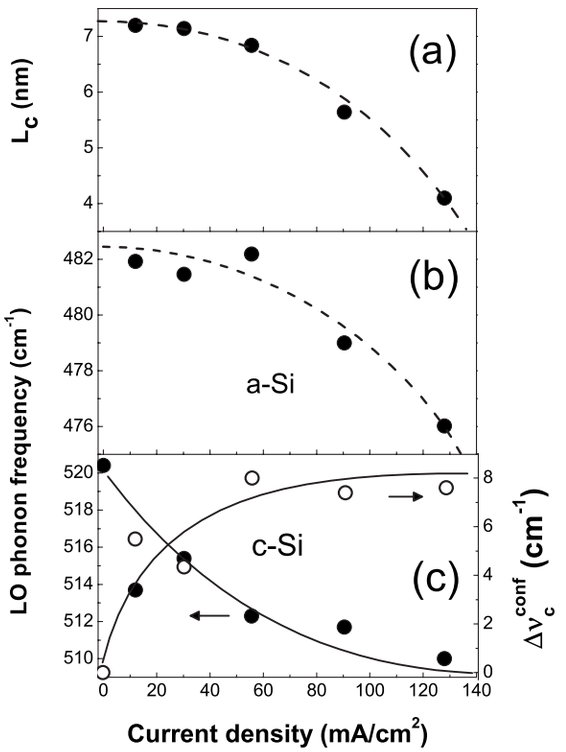

Figure 4. (a) LO phonon confinement lengths and frequencies of LO phonons corresponding to (b) crystalline and (c) amorphous phases, respectively, as determined for P-Si samples fabricated with different anodization current densities. Open circles in (c) are the strain-induced phonon shifts calculated in the crystalline phase. Lines are guides for the eyes.

increase in the a-Si volume with increasing current density/porosity (shown in the inset in Fig. 3). Moreover, the confinement of the LO phonons in the porous structure results in an asymmetry of the Raman line corresponding to c-Si. The average phonon confinement length ($L_c = 4.0$ nm) determined for this sample according to Ref. 5 may serve as an estimate of the characteristic size of the crystalline phase and it is found to be in reasonable agreement with the present SEM data. The phonon confinement length as a function of the anodization current density is shown in Fig. 4a. As expected, the increasing current density, i.e., increasing porosity, results in a decreasing L_c. The asymmetrical shape of the Raman line is fundamentally independent of stress, and linked to the characteristic size of the confinement region which determines the wavenumber of elementary excitations. Therefore, the obtained L_c may be straightforwardly associated with the average characteristic size of the crystalline domains.

Furthermore, as depicted in Fig. 4b and c, the LO frequencies of both crystalline and amorphous phases decrease with increasing current density. The data obtained in samples with different porosities follow monotonic dependences. The position of the Raman line corresponding to the crystalline phase measured in the sample fabricated with the lowest current density was found well below the expected value. This might be caused by the different pore arrangement in this sample, which may influence the average Raman response. To explain the behavior of the phonon frequencies, we analyze the internal strain distribution in the porous surfaces. According to the model proposed in Ref. 14, the amorphous phase covers the pore surface. Essential in this model is that the Si nanocrystal skeleton forming the P-Si is surrounded by the amorphous film that covers it. Because the a-Si film is considerably less dense than the c-Si,[20] the a-Si/c-Si interface is strained and a stress, nearly hydrostatic in character, results in the crystalline phase. Herewith, we

suppose that shifts of the phonon frequency in the amorphous phase are mainly determined by changes in strain, while those in the crystalline phase are subject to both strain and confinement effects. Assuming this model we can affirm that the a-Si is under compression, while the c-Si is under tension. Moreover, a relative variation of the amorphous and crystalline phase volumes influences the strain distribution. Namely, the model predicts that with the increasing a-Si to c-Si volume ratio, the amorphous phase relaxes, while the tensile strain of the crystalline phase increases. Using this model we were able to roughly estimate the contribution of the strain and confinement effects as follows: The ratio of the strain-induced frequency shifts of both phases ($\Delta\nu_{c(a)}^{strain}$) is inversely proportional to the thicknesses of the corresponding layers ($V_{c(a)}^{1/3}$), while the phase volumes determine the respective integral Raman intensities I_a. Consequently, we have

$$\frac{\Delta\nu_c^{strain}}{\Delta\nu_a^{strain}} \propto \left(\frac{V_a}{V_c}\right)^{1/3} \propto \left(\frac{I_a}{I_c}\right)^{1/3} \quad [1]$$

According to our data, in the sample with the highest porosity, $I_a/I_c \simeq 0.06$. Therefore, $\Delta\nu_c^{strain}/\Delta\nu_a^{strain} \simeq 0.4$. In this sample the strain-induced shift of the phonon frequency measured in the amorphous phase is about 6 cm^{-1}. Thus, the strain-induced phonon frequency shift in the crystalline phase is 2.4 cm^{-1}. The strain-induced phonon shifts calculated in this way for the samples with different porosities are shown in Fig. 4c. Finally, the contribution due to spatial confinement is given by $\Delta\nu_c^{conf} = \Delta\nu_c - \Delta\nu_c^{strain} \simeq 7.6$ cm^{-1}, where $\Delta\nu_c \simeq 10.0$ cm^{-1} is the phonon frequency shift in the crystalline phase observed in the sample with the highest porosity. Using the averaged dispersion of the longitudinal optical phonon in silicon,[21] we calculated the frequency shift in this sample caused by the phonon confinement as $\Delta\nu_c^{conf} \simeq 3.2$ cm^{-1}, with the experimentally obtained phonon localization length $L_c = 4.0$ nm determined by the asymmetry of the corresponding Raman line. Thus, the analysis of both the Raman line frequency position and the Raman line shape allowed us to independently determine the effect of the phonon confinement. The smaller phonon confinement frequency shift obtained from the shape of the Raman line is likely caused by the simplistic modeling of the rather complex Si porous structure in the form of columns according to Ref. 6. In spite of the crudeness of the assumptions involved in this analysis of the strain distribution, a reasonable agreement is found between the phonon frequency shifts due to the confinement ($\Delta\nu_c^{conf}$), obtained by both the Raman line peak position (effect of the strain included) and the line shape (not influenced by strain effect). This indicates the consistency of our model of the internal strain distribution in our P-Si samples.

In summary, Raman scattering by optical phonons was used to investigate the internal strain role in the determination of the LO phonon frequency in self-supported P-Si. Raman spectra reveal the existence of crystalline and amorphous phases. The increasing porosity is observed to cause (*i*) an increasing a-Si volume fraction, (*ii*) a redshift of the LO phonon frequencies in both (c-Si and a-Si) phases, and (*iii*) the enhanced asymmetrical broadening of the c-Si Raman line. A simple model considering the presence of the two lattice-mismatched crystalline and amorphous phases, which leads to their tensile and compressive stresses, respectively, is proposed. The analysis of the strain distribution among both phases shows that the increasing porosity results in a relaxation of strain in the amorphous phase and in the increasing strain in the crystalline phase of the P-Si. This leads to a considerable correction in the estimation of the characteristic size of the crystalline Si domains.

Acknowledgments

This work was performed within the framework of the Inter-American Collaboration in Materials (CIAM) research program. Financial supports from Brazilian agencies FAPESP and CNPq and Argentinean agency CONICET are gratefully acknowledged.

References

1. C. H. Arns, M. A. Knackstedt, W. Val Pinczewski, and E. J. Garboczi, *Geophysics*, **67**, 1396 (2002).
2. I. I. Reshina and E. G. Guk, *Semiconductors*, **27**, 401 (1993).
3. Y. Kanemitsu, H. Uto, Y. Matsumoto, T. Matsumoto, T. Fitagi, and H. Minura, *Phys. Rev. B*, **48**, 2827 (1993).
4. D. J. Lockwood, A. Wang, and B. Bryskiewicz, *Solid State Commun.*, **89**, 587 (1994).
5. H. Richter, Z. P. Wang, and L. Ley, *Solid State Commun.*, **39**, 625 (1981).
6. I. H. Campbell and P. M. Fauchet, *Solid State Commun.*, **58**, 739 (1986).
7. C. Ossadnik, S. Vepřek, and I. Gregora, *Thin Solid Films*, **337**, 148 (1999).
8. Y. Sun and T. Miyasato, *Jpn. J. Appl. Phys., Part 2*, **34**, L1248 (1995).
9. A. V. Andrianov, G. Polisski, J. Morgan, and F. Koch, *J. Lumin.*, **80**, 193 (1999).
10. D. Papadimitriou, J. Bitsakis, J. M. López-Villegas, J. Samitier, and J. R. Morante, *Thin Solid Films*, **349**, 293 (1999).
11. M. A. Ferrara, M. G. Donato, L. Sirleto, G. Messina, S. Santangelo, and I. Rendina, *J. Raman Spectrosc.*, **39**, 199 (2008).
12. I. M. Young, M. I. J. Beale, and J. D. Benjamin, *Appl. Phys. Lett.*, **46**, 1133 (1985).
13. D. Buttard, D. Bellet, and G. Dolino, *J. Appl. Phys.*, **79**, 8060 (1996).
14. R. R. Koropecki, R. D. Arce, and J. A. Schmidt, *Phys. Rev. B*, **69**, 205317 (2004).
15. J. M. Perez, J. Villalobos, P. McNeill, J. Prasad, R. Cheek, J. Kelber, J. P. Estrera, P. D. Stevens, and R. Glosser, *Appl. Phys. Lett.*, **61**, 563 (1992).
16. W. Theis, *Surf. Sci. Rep.*, **29**, 91 (1997).
17. S. Kasap, C. Koughia, H. Ruda, and R. Johanson, in *Springer Handbook of Electronic and Photonic Materials*, S. Kasap and P. Capper, Editors, Springer, New York (2006).
18. D. Bermejo and M. Cardona, *J. Non-Cryst. Solids*, **32**, 405 (1979).
19. Z. Iqbal and S. Veprek, *J. Phys. C*, **15**, 377 (1982).
20. J. C. Custer, M. O. Thomson, D. C. Jacobson, J. M. Poate, S. Roorda, W. C. Sinke, and F. Spaepen, *Appl. Phys. Lett.*, **64**, 437 (1994).
21. V. Paillard, P. Puech, M. A. Laguna, R. Carles, B. Kohn, and F. Huisken, *J. Appl. Phys.*, **86**, 1921 (1999).